

11-15-2002

Calculations of surface effects on phonon modes and Raman intensities of Ge quantum dots

Shang-Fen Ren
Illinois State University

Wei Cheng
Illinois State University

Follow this and additional works at: <http://ir.library.illinoisstate.edu/fpphys>

 Part of the [Condensed Matter Physics Commons](#)

Recommended Citation

Ren, Shang-Fen and Cheng, Wei, "Calculations of surface effects on phonon modes and Raman intensities of Ge quantum dots" (2002). *Faculty publications – Physics*. Paper 2.
<http://ir.library.illinoisstate.edu/fpphys/2>

This Article is brought to you for free and open access by the Physics at ISU ReD: Research and eData. It has been accepted for inclusion in Faculty publications – Physics by an authorized administrator of ISU ReD: Research and eData. For more information, please contact ISURed@ilstu.edu.

Calculations of surface effects on phonon modes and Raman intensities of Ge quantum dots

Shang-Fen Ren

Department of Physics, Illinois State University, Normal, Illinois 61790-4560

Wei Cheng

Institute of Low Energy Nuclear Physics, Beijing Normal University, Beijing 100875, Peoples Republic of China

(Received 29 June 2002; published 27 November 2002)

Phonon modes and Raman intensities of Ge quantum dots (QDs) with two different types of surfaces, a free standing surface or a fixed surface, in a size range from five atoms to 7 nm in diameter, are calculated by using a microscopic valence force field model. The results are compared, and the effects of surfaces on phonon properties of QDs are investigated. It is found that phonon modes and Raman intensities of QDs with these two different types of surfaces have obvious differences which clearly reveal the effects of the surfaces of QDs. The calculated results agree with existing experimental observations. We expect that our calculations will stimulate more experimental measurements on phonon properties and Raman intensities of QDs.

DOI: 10.1103/PhysRevB.66.205328

PACS number(s): 81.05.Cy, 63.22.+m, 02.20.-a, 78.30.-j

I. INTRODUCTION

Semiconductor quantum dots (QDs) have attracted much research attention in recent years because of their importance in the fundamental understanding and potential applications of electronic devices, information processing, and nonlinear optics.¹ Many optical, transport, and thermal properties of QDs are related to the phonon behavior in QDs. A clear theoretical understanding of these properties requires a reliable description of phonon modes and electron-phonon interactions in QDs.

So far, most of the theoretical understanding of phonon modes in QDs is based on continuum dielectric models. Analytic expressions of the eigenfunctions of LO phonons and surface optical phonons of small spherical²⁻¹⁰ and cylindrical¹¹ QDs were derived, and the electron-phonon interactions calculated. The extended continuum dielectric model,⁸⁻¹⁰ coupling the mechanical vibration amplitudes and the electrostatic potential, has made major improvements over classical dielectric models in the study of phonon modes in QDs. However, one of the basic assumptions of all dielectric models is that the material is homogeneous and isotropic, and this is valid only in the long wavelength limit. When the size of a QD is small, in the range of a few nanometers, the continuum dielectric models are intrinsically limited. On the other hand, one of the major difficulties in a microscopic modeling of phonon modes in QDs is its computational intensity. For example, for a Ge QD of about 8 nm, there are 11 855 atoms in it. Considering the three-dimensional motion of each atom, the dynamic matrix is in the order of 35 565. This is an intimidating task even with the most advanced computers.

In recent years, we have developed a microscopic valence force field model¹²⁻¹⁶ (VFFM) to study phonon modes in QDs by employing projection operators of irreducible representations of the group theory.¹⁷⁻²⁰ By employing group theory we can reduce the computational intensity dramatically. For example, the above matrix of size of 35 565 for QDs with 11 855 atoms can be reduced to five matrices in five different representations of A_1 , A_2 , E , T_1 , and T_2 , with

sizes of 1592, 1368, 2960, 4335, and 4560, respectively. Therefore, the original problem is reduced to a problem that can be easily handled by most reasonable computers. Furthermore, the employment of group theory proves to have played a much more important role than we expected. It not only allows the investigation of phonon modes in QDs of much larger sizes, but also it allows the investigation of phonon modes in QDs with different symmetries. These investigations led to many interesting physics that otherwise cannot be revealed.¹²⁻¹⁶ With this model, we have studied the size effects of phonon modes in semiconductor QDs, including QDs of one material, such as GaAs or InAs,¹²⁻¹⁴ as well as QDs with a core of one material embedded in a shell of another material, such as GaAs cores embedded in AlAs shells.¹⁵ We have also studied the size effects of Raman intensity in Si QDs.¹⁶

One thing we want to point out is that in all of our previous calculations, we used a free surface approximation, i.e., the atomic bonds at the surfaces were truncated and atoms at surfaces left with dangling bonds. To our knowledge, all other existing microscopic modelings on phonon modes in QDs also treated the surfaces in the same way.²¹⁻²³ We all know that this is far from the experimental reality in many circumstances. Surface effects on electronic and phonon properties of QDs have always been one of the major concerns in investigations of properties of QDs. The smaller the size of QDs, the larger the ratio of surface states to bulk states, the more important the surface of QDs.

In this work, we want to investigate the effects of different surfaces on phonon modes and Raman intensities of QDs. To achieve this goal, we have calculated phonon density of states (DOS) and Raman intensities of Ge QDs of different sizes with two different types of surfaces, one with free-standing surfaces as we did before, and another with fixed surfaces. These results of QDs with these two types of surfaces are calculated and compared, and the surface effects are analyzed and investigated. The results are also compared with the available experimental data, and our understanding of the fundamental physics are discussed.

This paper is organized as follows. In Sec. II, we describe

TABLE I. Phonon frequencies of bulk Ge at high symmetry points in the first Brillouin zone calculated by using the VFFM (Ref. 24) compared with the measured data (Ref. 30) (in brackets) in units of cm^{-1} .

Symmetry Points	LA	TA	LO	TO
Γ	0. (0.)	0. (0.)	300.9 (300.7)	300.9 (300.7)
X	79.9 (79.3)	216.1 (238)	216.1 (238)	282.7 (272.3)
L	56.5 (62.3)	176.5 (221)	243.7 (242.3)	292.0 (285)

our theoretical approaches briefly. In Sec. III, we show results of phonon DOS and present a discussion. In Sec. IV, we show results of Raman intensities and present a discussion. Section V is a summary.

II. THEORETICAL APPROACH

In our calculations, phonon modes in QDs are calculated by using the VFFM.²⁴ The details of the theoretical approaches were described in our previous publications.^{12–16} In this VFFM, only two parameters C_0 and C_1 , that describe the bond stretching and bond-angle bending forces, are introduced. The simplicity of this model allows us to focus attention on the fundamental physical properties of the systems. In calculations presented here C_0 and C_1 for Ge are taken as 47.2 and 0.845 eV, respectively.²⁴ The calculated results at high symmetrical points in the Brillouin zone for Ge bulk material are shown in Table I. For comparison, the experimental data are also listed in brackets. We can see that the agreements are reasonably good in general. On the other hand, because of its simplicity, this model cannot reproduce the entire phonon dispersion relation accurately. For example, the transverse acoustic phonon dispersion curve near the center of the Brillouin zone is not steep enough, and it is not flat enough near the boundary of the Brillouin zone. Keeping this in mind, we can better understand the calculated results of phonon properties of QDs.

After phonon modes are calculated by the VFFM, the Raman intensities of QDs are calculated by the bond polarizability approximation. This approach was described in detail in our previous work,¹⁶ so it will not be repeated here.

We treat QDs with free surfaces the same as we did before.^{12–16} For QDs with fixed surfaces, we could rewrite our computer programs to calculate their phonon modes exactly. However, since we have existing computer programs to calculate phonon modes in QDs with a core/shell structure,¹⁵ we take an easy approach in the following. We use the core/shell QD model and make the core a Ge QD. Then we take the mass of atoms in the external shell to be 1000 times the mass of the Ge atoms, and take the thickness of the external shell to be more than 0.3 nm. The large mass of atoms in the external shell ensures that the interface between the core and shell is well fixed, and the thickness of the shell is larger than the Ge bond length, which ensures that no dangling bond of Ge atoms is left at the surface of the QDs.

III. PHONON DOS

We have calculated phonon modes in Ge QDs with two different types of surfaces, a free standing surface or a fixed

surface, in a size range from five atoms up to about 7 nm in diameter. Then the DOS, $D(\omega)$, is calculated by the Lorentz broadening

$$D(\omega) = \sum_i \frac{n_i \Gamma / \pi}{(\Gamma)^2 + (\omega - \omega_i)^2},$$

where ω_i is an eigenfrequency, n_i is its number of degeneracy, which is one for A_1 and A_2 modes, two for E modes, and three for T_1 and T_2 modes, and Γ is the half Lorentz width, which is taken as 0.5 cm^{-1} in our calculations. The summation runs over all phonon modes.

The DOS of QDs with these two types of surfaces with a few sizes are shown in Fig. 1. The left panel is for QDs with a fixed surface, and the right panel if for QDs with a free surface. Comparing these results we notice that there are more low frequency peaks in QDs with free surfaces than in QDs with fixed surfaces. This is very obvious when the size of a QDs is less than 3 nm. When the size of a QDs increases, the DOSs of QDs with these two different surfaces

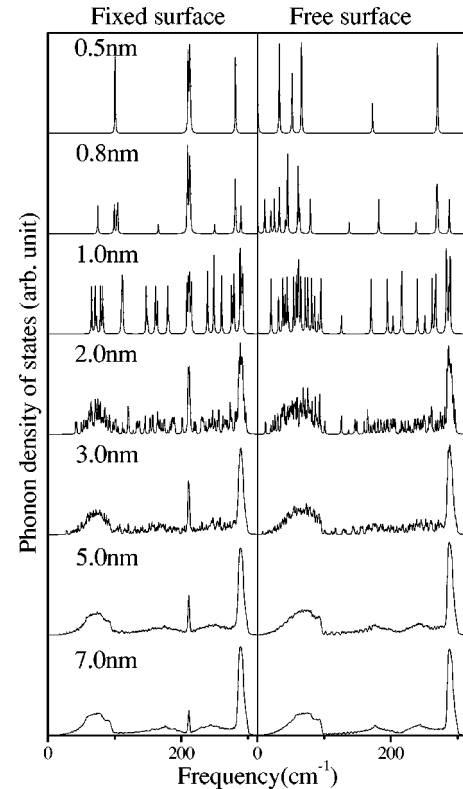


FIG. 1. Calculated total phonon DOS for Ge QDs, with fixed or free surfaces of approximate sizes (diameters) indicated in nm.

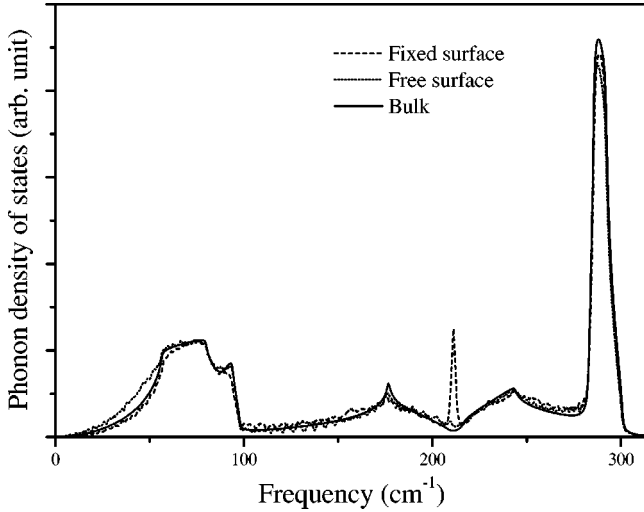


FIG. 2. Calculated total phonon DOS for Ge bulk material and QDs with fixed or free surfaces of about 7.0 nm in diameter.

both approach that of bulk. One major feature of phonons in QDs with fixed surfaces is that there is always a major peak at the frequency of about 211 cm^{-1} , which corresponds to the frequency range between the optical and acoustic phonons of the bulk Ge. This peak represents interface phonons, which is still strong in QDs of 7 nm, the maximum size of our present calculations.

To compare our results with the bulk phonon DOS carefully, we plotted the DOSs of QDs with two different types of surfaces and bulk material together. In Fig. 2, the solid line is for the DOS of Ge bulk material, and the dashed and dotted lines are for QDs of 7 nm with fixed and free surfaces, respectively. Comparing to the bulk phonon DOS, the major difference in the DOSs of QDs with fixed surfaces is the existence of an interface phonon peak, and the DOSs of QDs with free surfaces are obviously higher than that of Ge bulk material in the low frequency range. For the major optical peak, the DOSs of both types of QDs are lower than that of bulk, with a slightly redshift of the frequency. This is more obvious for DOSs of QDs with free surfaces. Both the differences in the low frequency range and in the major optical peak indicate the influence of surface effects on phonon modes in the long wavelength range of the bulk material. The longer the wavelength, the more sensitive it is to the surface differences. Some of these features will be discussed next.

IV. RAMAN INTENSITIES

We have calculated Raman intensities of QDs with two different types of surfaces with approximate diameters between 0.5 and 7.0 nm. Again the Raman intensity I is calculated by the Lorentz broadening

$$I = \sum_l \frac{I_l \Gamma / \pi}{(\Gamma)^2 + (\omega - \omega_l)^2},$$

where I_l and ω_l are the scattering intensity and eigenfrequency of mode l , respectively, and Γ is the half Lorentz

TABLE II. Raman intensities of T_2 modes for Ge QDs with two different surfaces, a free surface or a fixed surface, with approximate sizes of 1.0, 2.0, 3.0, 4.0, 5.0, 6.0, and 7.0 nm. The data listed in order are the diameters of the QDs (d), the number of atoms in the QDs (N), the frequency of the highest peak of T_2 [$\omega_{T_2}(\text{free})$], and the integrated intensity of T_2 modes [$I_{T_2}(\text{free})$] of QDs with free surfaces, and the same two quantities. All intensities listed are Raman intensity per atom.

d (nm)	N	$\omega_{T_2}(\text{free})$	$I_{T_2}(\text{free})$	$\omega_{T_2}(\text{fix})$	$I_{T_2}(\text{fix})$
0.934	29	289.0	0.9507	290.9	0.2286
1.952	167	296.6	0.6387	297.1	0.2286
2.914	633	299.1	0.5077	299.2	0.2286
3.985	1503	299.9	0.4361	300.0	0.2286
4.977	2917	300.3	0.3995	300.3	0.2286
5.983	5011	300.5	0.3707	300.5	0.2286
6.993	8105	300.6	0.3524	300.6	0.2286

width, which is taken as 0.5 cm^{-1} in our calculations. Following our previous work,¹⁶ Raman intensities of A_1 , E , and T_2 modes for each QD are calculated and investigated.

We notice from our results that even though the size effects on the strengths of Raman peaks of Ge QDs with free surfaces are very similar to those discussed in our previous work,¹⁶ the size effects on strengths of Raman peaks of QDs with fixed surfaces are obviously different. In general, the Raman strengths of QDs with fixed surfaces are more similar to those of the bulk material, but they also have unique features. These will be discussed in detail next.

We have listed related important data in Table II that are numerically more accurate. The data listed in order are the diameters of the QDs calculated (d), the number of atoms in the QDs (N), the frequency of the highest peak of the T_2 mode [$\omega_{T_2}(\text{free})$] and the integrated intensity of T_2 modes [$I_{T_2}(\text{free})$] of QDs with free surfaces, and the same two quantities of QDs with fixed surfaces [$\omega_{T_2}(\text{fix})$ and $I_{T_2}(\text{fix})$]. For easier comparison, all intensities listed above are Raman intensity per atom. The important features of these results will be discussed next.

A. Size effects on strengths of the Raman peaks

All Raman intensities in three different symmetries A_1 , E , and T_2 , of QDs with two different surfaces and different sizes, are calculated and investigated. It is found that the size effects on the total strengths of Raman peaks for Ge QDs with free surfaces are similar to those of Si QDs studied before,¹⁶ but it is different for QDs with fixed surfaces. It is found that in general the Raman strengths of A_1 and E modes in QDs with fixed surfaces are much smaller than those in QDs with free surfaces, with a ratio of the order of 10^{-11} . This indicates that the A_1 and E Raman intensities in QDs with fixed surfaces can be ignored with the computational accuracy considered, which is similar to the Raman intensities of bulk materials. This is the reason that corresponding numbers of A_1 and E intensities are not listed in Table I. They are too small to be considered seriously. Not only is this true for A_1 and E modes, but it also is true for T_2 modes

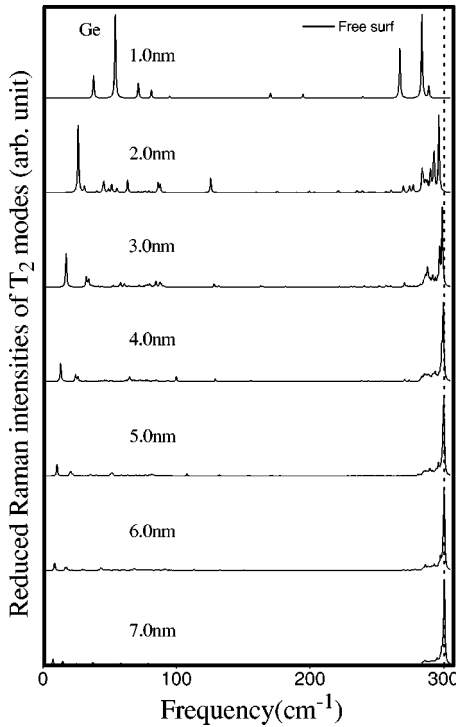


FIG. 3. Reduced Raman intensities of T_2 modes for Ge QDs with free surfaces of approximate diameters indicated in nm.

in the low frequency range. Because of this, there is no obvious Raman peaks in A_1 and E modes for QDs with fixed surfaces, and there is no obvious Raman peaks in the low frequency range of T_2 modes. In Figs. 3 and 4, the Raman intensities of T_2 modes for QDs with two different surfaces and different sizes are shown. From these two figures and the DOSs shown above, we learned that Raman peaks at the lower frequency range in Fig. 3 are caused by the free surfaces of QDs. Similarly, all the low frequency Raman peaks in A_1 , E , and T_2 in QDs with free surfaces, that were shown in Figs. 1–3 of Ref. 16, are also caused by the free surfaces of QDs. On the other hand, for QDs with fixed surfaces, the low frequency property are more similar to that of a bulk material, i.e., the low frequency Raman peaks can be ignored in QDs with fixed surfaces.

Since experimentally the presence of multiple Raman peaks as shown in Figs. 3 and 4 may not be resolvable due to size fluctuation (instead a broadened peak is observed), we have also integrated all the Raman intensity for each QD to obtain the total strength of the Raman peaks. To do this we have summed the calculated Raman intensities (without broadening) for all A_1 , E , and T_2 modes respectively, for QDs with different sizes. Our result show that for QDs with fixed surfaces, the total Raman intensities of A_1 and E modes are very small (10^{-12}) comparing to the total strengths of T_2 modes (10^{-1}), and the integrated Raman intensities of T_2 modes remain almost exactly as a constant (see Table II). This is different from the total Raman intensities of QDs with free surfaces,¹⁶ but agrees with the bulk material. Thus, we understand that the increase of total Raman intensities in small QDs with free surfaces is mainly caused by the free surfaces of QDs.

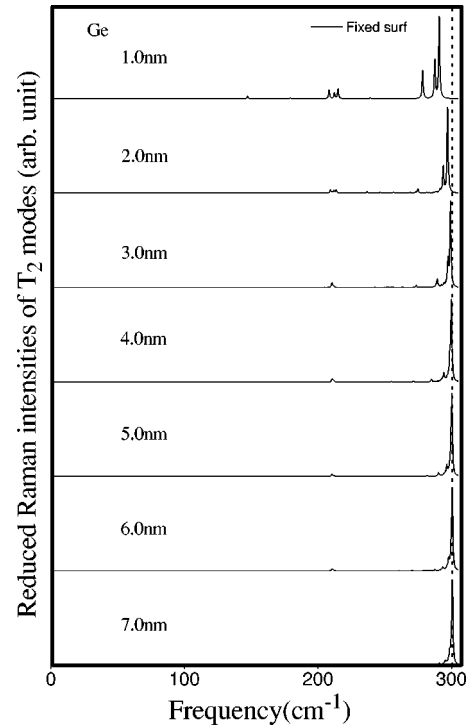


FIG. 4. Reduced Raman intensities of T_2 modes for Ge QDs with fixed surfaces of approximate diameters indicated in nm.

B. Size effects of highest frequencies

From our results, we know that, in general, major peaks in the high frequency range of QDs with both types of surfaces always have a T_2 symmetry, which corresponds to T_2 phonon modes with the highest frequencies. When the size of the QDs increases, this frequency approaches the frequency of the bulk optical phonon frequency. Theoretically speaking, when the size of QDs approaches infinity, the total Raman spectrum of QDs approaches the Raman spectrum of bulk Ge, and this will be the only peak left. From Figs. 3 and 4, we see that this is true for QDs with both types of surfaces. When the sizes of QDs decrease, the frequency of this T_2 peak decreases, due to the confinement of optical phonons in QDs with both types of surfaces. To show this more clearly, we have enlarged the high frequency range of Figs. 3 and 4 and plotted them together in Fig. 5. In Fig. 5, the solid lines are for QDs with fixed surfaces and the dashed lines are for QDs with free surfaces. The frequency of the optical phonons at the center of the bulk Brillouin zone in our model is 300.9 cm^{-1} , which is shown as a vertical dashed line in Fig. 5. The frequency of the highest Raman peak for different QDs are listed in Table II. From Fig. 5 and Table II, we see that when the sizes of the QDs are the same, the shifts of the frequency of the highest Raman peak for QDs with different surfaces are quite similar. When diameters of Ge QDs are less than 4 nm, the frequencies of the highest Raman peaks in QDs with free surfaces are slightly lower than those in QDs with fixed surfaces. This systematic redshift of phonon peaks due to spatially confined phonon modes in nanocrystals in the size range of a few nm have been observed,^{25–27} and recently it was observed by resonant Ra-

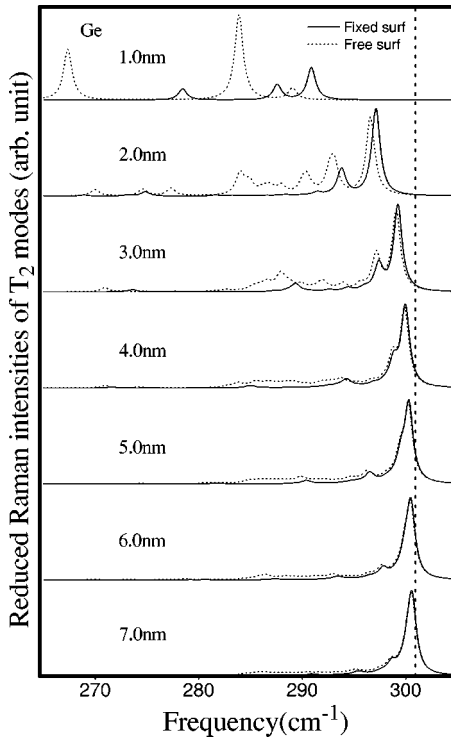


FIG. 5. Reduced Raman intensities of T_2 modes enlarged at the high frequency range for Ge QDs with approximate diameters indicated in nm. The solid lines are for QDs with fixed surfaces, and the dashed lines are for QDs with free surfaces.

man scattering in three samples of Ge nanocrystals in the size range of 4–10 nm.²⁸ From our calculations of QDs with two different types of surfaces, we conclude that this is a true quantum confinement effect. From Figs. 3–5 we also see that Raman intensities for QDs with free surfaces have a broader tail of peaks, and the corresponding ones for QDs with fixed surfaces have fewer peaks. This tells us that some of these peaks are caused by vibrations of atoms near the free surfaces.

Another thing we notice from Figs. 3–5 is that, for high frequency peaks of T_2 modes, not only does the highest intensity peak redshift as the dot size decreases, but weaker peaks appear at the same time. This is true for QDs with both types of surfaces. Experimentally it may be difficult to resolve all the weaker peaks because of the broadening resulting from the fluctuation in dot sizes. Therefore, one may observe an asymmetric broadening of the Raman peak corresponding to the optical phonon as the dot size is reduced. This was indeed found in Raman intensities of Ge QDs.²⁹ As we pointed out in our previous work, one may attempt to interpret the asymmetrical broadening of Raman peaks in experimental observations as an indication that the quality of the dots may be poorer; thus it leads to larger inhomogeneous broadening at lower frequencies. However, from our calculations of Raman intensities of QDs, we notice that the redshift of the strongest T_2 Raman peak is smaller than the frequency spread of the weaker peaks which appear. In other words, the broadening of the Raman peak is larger than the redshift as the dot size decreases. This is true for QDs with both types of surfaces. This indicates that the observed

broadening in Raman measurements is not only due to the redshift of the major peak alone, but there could be a major contribution to the broadening from the quantum size effects.

C. Size effects of lowest frequencies and folding of the acoustic phonons

As we discussed above, in the low frequency range the Raman intensities of QDs with free surfaces are similar to what we discussed in detail in our previous work. For example, there is a folding of the acoustic phonons for A_1 modes in the low frequency range, as shown in Fig. 1 of Ref. 16. But the Raman intensities for QDs with fixed surfaces are too small to discuss. This indicates that a folding of A_1 acoustic phonons in QDs with free surfaces is caused by the free surfaces, which is different from our original understanding.

D. Existence of a Raman peak of interface modes for QDs with fixed surfaces

One unique feature we notice in the Raman strength of QDs with fixed surfaces is that there exists a Raman peak at the frequency of about 211 cm^{-1} in QDs of all different sizes. We have noticed that there is a major peak at the same frequency range for DOSs of all QDs with fixed surfaces, as shown in Fig. 1, and we have discussed the interface feature of these modes in Sec. III.

To study the interface modes more carefully, we have employed the concept of the average vibration amplitude¹³ to investigate it. The average vibration amplitude A_l^i of the l th shell in the i th phonon mode is defined as

$$A_l^i = \frac{1}{n} \sum_{k=1}^n |a_{lk}^i|, \quad (4.1)$$

where a_{lk}^i is the vibration amplitude of the atom k in the l th shell in the i th phonon mode, and n is the total number of atoms in the l th shell. In Fig. 6, we show the average vibration amplitudes of the T_2 mode with a frequency of 210.5 cm^{-1} in 6.0-nm (diameter) QDs with fixed surface. From the above figures we believe that this is an interface mode. From Fig. 6 we see that obviously the vibration amplitudes of this mode is small in the internal region of the QD, but very large near the interface. This indicates that this is indeed an interface mode. For comparison, we have also plotted the average amplitudes of the T_2 mode with the highest frequency of 300.5 cm^{-1} for the same QD. This is a confined optical mode, as we discussed in previous work.¹³

V. SUMMARY

In summary, we have calculated phonon DOSs and Raman intensities of Ge QDs with two different types of surfaces. The results are compared with each other, and with the experimental data and properties of the bulk material. It is found that when the sizes of QDs is large, such as 7 nm, the DOSs of phonon modes of QDs with fixed surfaces are similar to that of bulk material, except for the existence of a sharp peak that corresponds to interface modes. The DOSs of

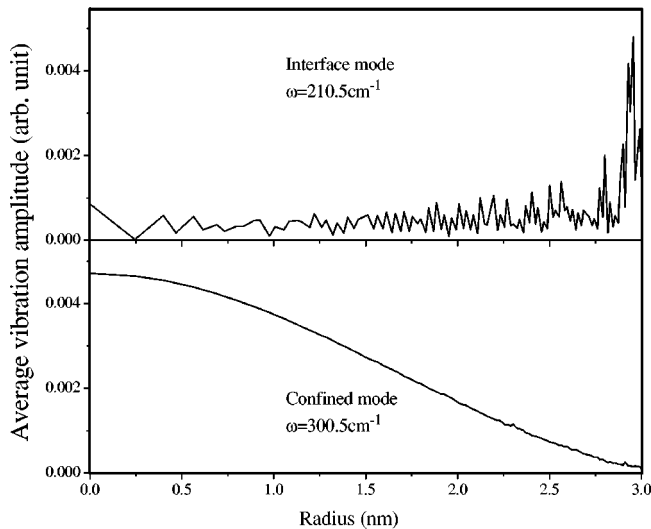


FIG. 6. Average vibration amplitudes for two T_2 modes in a 6.0-nm (diameter) QD with a fixed surface. The above amplitude has a frequency of 210.5 cm^{-1} which is an interface mode, and the second one has a frequency of 300.5 cm^{-1} which is a confined optical mode.

QDs with free surfaces are similar to those of a bulk material, but there is obvious difference in the low frequency range. For Raman intensities, the results of Ge QDs with free surfaces are qualitatively similar to those of Si QDs that we discussed above, but the results of Ge QDs with fixed surfaces are quite different.

In the latter, the Raman intensities in the acoustic frequency range are similar to those of the bulk material, and in the high frequency range there exist two different types of Raman peaks: one caused by the confined optical modes, and another caused by the interface between the QDs and the external material. The first type has the same behavior as those in QDs with free surfaces, with similar redshifts as the size decreases. The interface phonons in a frequency range between the acoustic and optical phonon frequency range of bulk Ge are unique for QDs with fixed surfaces. The comparison of results of the Raman intensities in QDs with these two different surfaces reveals the surface effects on Raman intensities of QDs. In our theoretical calculations, we have considered these two different surfaces which are two extreme cases, i.e., the free standing surface corresponds to extremely light surface atoms and the fixed surface corresponds to extremely heavy surface atoms. In real QDs that are fabricated and observed in experiments, in most situations the surface of QDs will be somewhere in between. Our calculated results agree well with the existing experimental observations, and we expect that our calculations can stimulate more experimental measurements of related properties of QDs.

ACKNOWLEDGMENT

This research was supported by the National Science Foundation (INT0001313). We want to thank Professor W. A. Harrison and Professor P. Y. Yu for helpful discussions.

- ¹A.D. Yoffe, *Adv. Phys.* **42**, 173 (1993); **50**, 1 (2001).
- ²E. Duval, *Phys. Rev. B* **46**, 5795 (1992).
- ³M.C. Klein, F. Hache, D. Ricard, and C. Flytzanis, *Phys. Rev. B* **42**, 11 123 (1990).
- ⁴H. Frohlich, *Theory of Dielectrics, Dielectric Constants, and Dielectric Loss* (Oxford University Press, New York, 1949).
- ⁵R. Fuchs and K.L. Kliewer, *Phys. Rev.* **140**, A2076 (1965).
- ⁶R. Ruppin and R. Englman, *Rep. Prog. Phys.* **33**, 144 (1970).
- ⁷C. Trallero-Giner, F. Garcia-Moliner, V.R. Velasco, and M. Cardona, *Phys. Rev. B* **45**, 11 944 (1992).
- ⁸E. Roca, C. Trallero-Giner, and M. Cardona, *Phys. Rev. B* **49**, 13 704 (1994).
- ⁹M.P. Chamberlain, C. Trallero-Giner, and M. Cardona, *Phys. Rev. B* **51**, 1680 (1995).
- ¹⁰C. Trallero-Giner, A. Debernardi, M. Cardona, E. Menendez-Proupin, and A.I. Ekimov, *Phys. Rev. B* **57**, 4664 (1998).
- ¹¹W.S. Li and C.Y. Chen, *Physica B* **229**, 375 (1997).
- ¹²S.F. Ren, Z.Q. Gu, and D. Lu, *Solid State Commun.* **113**, 273 (2000).
- ¹³S.F. Ren, D.Y. Lu, and G. Qin, *Phys. Rev. B* **63**, 195315 (2001).
- ¹⁴G. Qin and S.F. Ren, *J. Appl. Phys.* **89**, 6037 (2001).
- ¹⁵G. Qin and S.F. Ren, *Solid State Commun.* **121**, 171 (2002).
- ¹⁶W. Cheng and S.F. Ren, *Phys. Rev. B* **65**, 205305 (2002).
- ¹⁷S.Y. Ren, *Phys. Rev. B* **55**, 4665 (1997).
- ¹⁸S.Y. Ren, *Solid State Commun.* **102**, 479 (1997).
- ¹⁹S.Y. Ren, *Jpn. J. Appl. Phys.* **36**, 3941 (1997).
- ²⁰S.Y. Ren and S.F. Ren, *J. Phys. Chem. Solids* **59**, 1327 (1998).
- ²¹J. Zi, H. Buscher, C. Falter, W. Ludwig, K. Zhang, and X. Xie, *Appl. Phys. Lett.* **69**, 200 (1996).
- ²²J. Zi, K. Zhang, and X. Xie, *Phys. Rev. B* **58**, 6712 (1998).
- ²³H. Fu, V. Ozolins, and A. Zunger, *Phys. Rev. B* **59**, 2881 (1999).
- ²⁴W.A. Harrison, *Electronic Structures and the Properties of Solids* (Freeman, San Francisco, 1980).
- ²⁵P.T.C. Freire, M.A. Araujo Silva, V.C.S. Reynoso, A.R. Vaz, and V. Lemos, *Phys. Rev. B* **55**, 6743 (1997).
- ²⁶Y.N. Hwang, S. Shin, H.L. Park, S.H. Park, U. Kim, H.S. Jeong, E.J. Shin, and D. Kim, *Phys. Rev. B* **54**, 15 120 (1996).
- ²⁷A. Balandin, K.L. Wang, N. Kouklin, and S. Bandyopadhyay, *Appl. Phys. Lett.* **76**, 137 (2000).
- ²⁸K.L. Teo, S.H. Kwok, P.Y. Yu, and S. Guha, *Phys. Rev. B* **62**, 1584 (2000).
- ²⁹P.Y. Yu (private communication).
- ³⁰G. Nilsson and G. Nelin, *Phys. Rev. B* **6**, 3777 (1972).